

中国激光

全脑显微光学成像

江涛^{1,2}, 龚辉^{1,2}, 路清铭^{1,2,3}, 袁菁^{1,2*}

¹华中科技大学苏州脑空间信息研究院, 江苏 苏州 215000;

²华中科技大学武汉光电国家研究中心, 湖北 武汉 430074;

³海南大学生物医学工程学院, 海南 海口 570228

摘要 全脑介观神经联接研究是解析脑认知功能的神经输入输出环路结构基础、普查基因表达与细胞类型, 以及绘制全景立体脑图谱的科学前沿。光学成像方法在横向方向能够达到亚微米的分辨率, 并可通过多种手段实现“光学切片”的效果, 具备在介观水平观测神经环路的天然优势。基于组织透明或机械切削的自动化全脑显微光学成像方法, 突破了光学成像在生物组织中成像深度的限制, 具有在大范围内提供介观水平精细观察的技术优势。结合各类生物样本荧光标记技术, 全脑显微光学成像方法在神经环路的结构和功能的研究方面有着巨大潜力, 已成为剖析全脑神经及血管网络的最佳方式。为了更全面地了解和认识这种有力的工具, 总结了近年来发展的各类全脑显微光学成像方法, 并展望了未来的技术发展。

关键词 生物光学; 全脑显微光学成像; 光学层析; 微米分辨率; 脑图谱; 神经环路; 神经元

中图分类号 Q-334

文献标志码 A

DOI: 10.3788/CJL221247

1 引言

大脑是自然界最复杂的系统之一, 是生命诞生数十亿年以来进化的巅峰。人类一直希望能够破译大脑运转密码、揭开生命之谜, 但时至今日我们仍无法准确描述记忆、思维和意识的产生机制。由于对脑的结构和功能缺乏认识, 导致对精神分裂症、癫痫、阿尔兹海默症和帕金森氏病等神经系统疾病缺乏有效的干预药物和治疗手段; 脑疾病已经成为社会负担最重的病种。另一方面, 对脑认识的不足也阻碍了以神经科学研究结果为基础的人工智能技术的发展。因此, 脑科学备受各国政府的重视, 近年来, 全球范围的脑科学竞争已经进入白热化状态。在人类基因组计划之后, 阐明大脑的结构和功能是目前最具挑战性的研究课题之一^[1]。

脑的结构极其复杂, 按不同物理尺度可以将脑分为脑叶、神经环路、神经元、突触甚至分子等层次。脑的强大功能源于其数量巨大的神经细胞及其复杂的相互联接。神经环路是由大量不同神经元有机组合形成的、实现特定信息传递与处理的结构功能单位, 是实现脑高级功能的基本单元。复杂的脑功能需要多个脑区的共同参与, 并由局部和长程神经环路共同协同作用^[2]。神经系统疾病往往伴随着功能相关的特定神经环路及其输入联接与输出投射关系的结构异常。神经

元是神经环路的基本组成单元, 人脑中约有 860 亿个神经元, 而作为神经科学研究中经典的模式动物之一, 小鼠脑中约有 7000 万个神经元^[3]。神经元突触的大小仅约 1 μm 甚至更小, 典型神经元胞体的直径为 10~30 μm, 神经纤维的直径仅为数百纳米至 1 μm^[4]; 而神经元的树突可覆盖局部数百微米的范围, 轴突的长度则可延伸至更远的位置甚至达到全脑范围。由此可见, 脑神经联接结构的研究同时具备了大范围和跨尺度两个特点, 研究脑神经联接结构就像绘制世界地图, 既需要覆盖世界范围, 又需要精确到每个国家的基层路网等局部细节。

神经联接图谱的绘制与研究是阐明脑认知功能的重要神经基础, 是发展类脑智能、探讨认知障碍相关重大脑疾病发病机制、理解儿童和青少年脑智发育的科学基础, 也是发展新技术新方法的源动力。“脑地图”的绘制已经有一百多年的历史, 从 1906 年的诺贝尔奖得主、西班牙科学家 Cajal 绘制神经细胞图谱(奠定了现代神经科学的基础), 到德国解剖学家 Broadman 将大脑划分为 52 个不同的区域, 再到 20 世纪后半叶于利希研究所把人脑划分为 120 多个分区, 都极大地促进了脑科学的研究发展。2009 年美国启动了基于功能磁共振成像技术的人脑连接组计划, 2016 年又启动了基于电镜技术的大脑皮层网络的机器智能计划(MICrONS, 也称大脑“阿波罗计划”)。这些都是对

收稿日期: 2022-09-15; 修回日期: 2022-10-10; 录用日期: 2022-10-18; 网络首发日期: 2022-11-04

基金项目: 科技部科技创新 2030 重大项目(2021ZD0201000)、国家自然科学基金(81827901)

通信作者: *yuanj@hust.edu.cn

“绘制脑地图”的尝试,但它们都尚不能在全脑范围内展示出单个神经元的精细结构。

“工欲善其事,必先利其器”,针对小鼠等模式动物的全脑介观神经联接图谱绘制,需要有能够规模化地获取全脑尺度范围高分辨率三维数据的技术工具。在微观层次,电子显微镜(EM)的分辨率高达纳米水平,能够观察细胞亚显微结构,如直径仅几十纳米的突触小泡;但受限于扫描速度,电子显微镜适用的样本尺寸通常只有毫米水平,无法实现对厘米尺寸小鼠全脑的超高分辨率三维成像。在宏观层次,电子计算机断层扫描(CT)和磁共振成像(MRI)可以获得从数厘米尺寸完整器官到整个人体的解剖结构信息;然而其分辨率目前只有毫米量级,不足以解析单细胞水平的精细结构。在介观层次,光学成像方法的横向分辨率可达

亚微米的水平,能够分辨胞体、轴突和树突等结构,具备观测神经环路精细结构的天然优势。同时,通过共聚焦、结构光和双光子激发这类“光学切片”^[5-7]技术能够方便地实现层析成像,通过受激辐射损耗显微术、结构照明显微术和单分子定位显微术可突破光学衍射极限实现超分辨显微成像^[8-9],还可与数据驱动的深度学习方法结合进一步突破传统光学显微镜的功能和性能的边界^[10]。但由于生物组织对光的散射和吸收,导致这些传统光学方法的成像深度有限,仅能对鼠脑浅层数十微米至数百微米部分进行成像。为了突破光学成像方法在生物组织中成像深度的限制,实现高像素分辨率和大范围的三维探测,光学显微镜必须和组织学方法结合起来,以实现全脑范围精细结构的三维重现。总的来说,全脑显微光学成像的技术路径大致如图1所示。

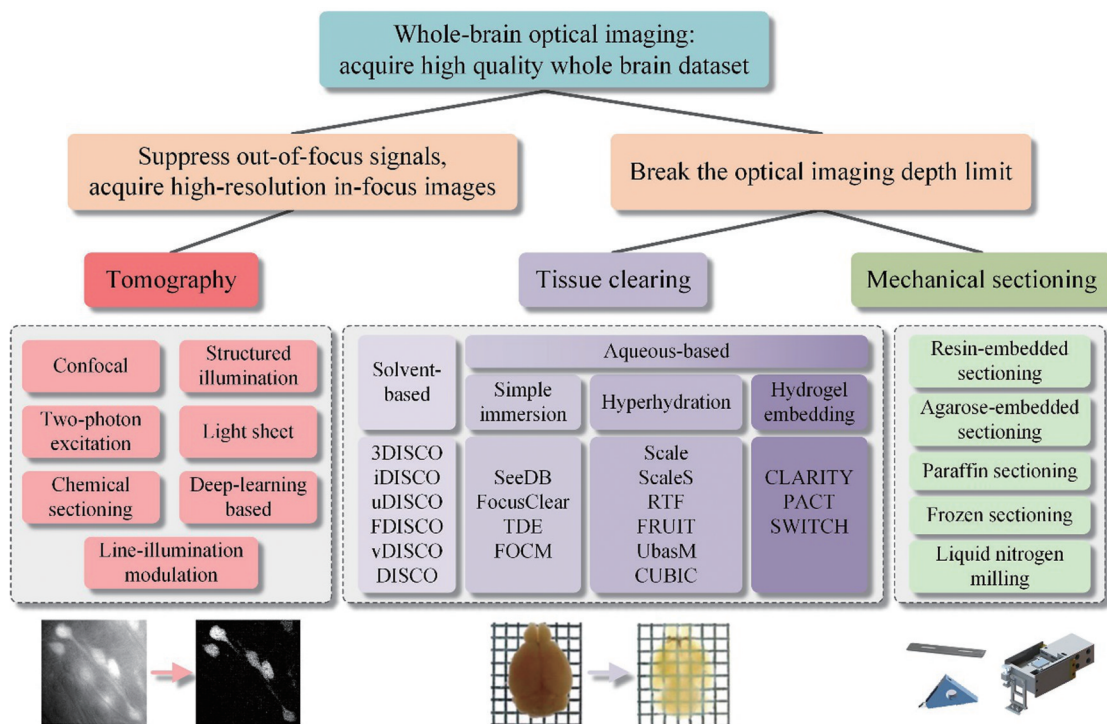


图1 全脑显微光学成像的技术路径
Fig. 1 Technical pathways for whole-brain optical imaging

近十年来,全球多个研究中心都在推动脑计划相关研究:欧盟将脑科学纳入未来新兴技术旗舰计划;2013年美国总统奥巴马提出“创新性神经技术推动的脑研究”;日本推出了以灵长类动物为模型的脑计划。我国也一直积极部署神经科学相关的重大科技项目^[11]并启动了科技创新2030“脑科学与类脑研究”重大项目。在此研究背景下,各种基于不同光学成像原理与实现方式的全脑显微光学成像方法不断涌现,结合各类生物样本荧光标记、数据处理与可视化技术形成配套的完整解决方案,可获得兼具介观分辨率和大尺度范围的三维精细结构等信息,为回答重要的生物学问题提供关键依据,已逐渐成为剖析全脑神经网络的最佳方式^[12]。例如,针对模式动物的介观脑联接图

谱研究,可进行全脑任意脑区的神经元精细形态分析、胞体定量分析、神经投射路径分析^[13-16];绘制全脑立体定位三维脑图谱,对全脑所有的区域进行划分和标注,为各项研究提供脑空间定位的基准坐标参考^[17-20];绘制脑血管联接图谱,为血管疾病相关的发病机理研究和药物研发提供形态测量学依据^[21-27];绘制不同脑区特定类型神经元的空间分布图谱及输入输出图谱,实现单细胞水平的神经环路解析^[28-33],为揭示脑的结构组织规律和神经信息处理机制提供重要信息。这些工作的开展都显示出人们开始认识到介观层面解析神经环路在脑研究中的重要性。

然而,为获得整体一致、覆盖数厘米范围、分辨率达到微米甚至亚微米水平的全脑三维数据集,需要考

虑和平衡许多技术参数,如各向同性分辨率、成像范围、成像时间、系统鲁棒性、图像自动配准和成本等。在此,我们将回顾全脑显微光学成像技术的最新进展,并对未来的技术发展与挑战做出展望。

2 基于组织透明的全脑显微光学成像方法

基于组织透明的全脑显微光学成像方法是指先将生物组织进行光透明化处理^[34-35]以提升光学成像深度,然后再用光片荧光显微镜(LSFM)进行快速成像的技术。生物组织对光的散射是由于不同部位的折射率不一致所引起的,例如细胞膜中脂质的折射率明显高于细胞内外水分的折射率^[36-37],光在穿过细胞膜时就会产生散射现象。因此,为实现样本的光透明化,需使得样本内各部分的折射率一致。早在 20 世纪初,Spalteholz^[38]就发明了一种利用有机溶剂使得完整器官变透明的方法。近些年来出现了大量的组织透明处理方法,通过不同的手段来减少光在组织中的散射,从而实现样本的光透明化。总的来说,各种不同的组织透明方法可大致分为两类:一类为基于有机溶剂的方法,另一类为基于亲水性试剂的方法。

基于有机溶剂的组织透明方法主要分为两大步骤:脱水和折射率匹配^[39]。脱水操作使用脱水试剂去除组织中低折射率的水,同时也带走组织中一部分高折射率的脂质成分。折射率匹配操作是通过高折射率、高渗透率的溶液浸泡脱水后的组织,使其快速填充到组织中,最终达到组织中各部分折射率基本均匀的透明状态。基于有机溶剂的组织透明方法有 3DISCO^[40-41]技术、iDISCO^[42]技术、uDISCO^[43]技术、FDISCO^[44]技术、vDISCO^[45]技术、sDISCO^[46]技术和 PEGASOS 技术^[47]。总体而言,基于有机溶剂的组织透明方法具有透明速度快、透明程度高的优点,但同时也存在内源荧光信号易淬灭和组织变形较大的缺点,不利于后期图像数据的配准以及数据分析。

基于亲水性试剂的组织透明方法可分为三类:(1)基于简单浸泡的组织透明方法;(2)基于组织水合的组织透明方法;(3)基于水凝胶包埋的组织透明方法。基于简单浸泡的组织透明方法是指通过高折射率的水溶性试剂直接浸泡组织,使得组织各部分的折射率相对均匀,实现组织整体光透明化,代表性的方法有 SeeDB^[48-49]、FocusClear^[50]、TDE^[51]和 FOCM^[52]等。该类方法操作简单,但透明效果较差,很难应用在成年鼠脑这种大体积组织的透明成像上。基于组织水合的组织透明方法是指通过水合作用去除组织中的致密胶原纤维,并通过高折射率试剂使组织中各部分折射率匹配,代表性方法有 Scale^[53]技术、ScaleS^[54]技术、RTF^[55]技术、FRUIT^[56]技术和 UbasM^[57]技术等。这些方法未能去除组织中的脂质,所以透明效果有限,难以应用在完整的鼠脑组织上。另外一些方法在水合作用的基础上

上,使用特定试剂去除了组织中的脂质,可实现成年小鼠全脑的光透明化,典型代表有 CUBIC^[58-59]技术,但该方法需要较长的处理时间。基于水凝胶包埋的组织透明方法是通过水凝胶包埋固定组织中的蛋白质,然后通过电泳等主动或者被动的方式去除组织中的脂质,最终达到光透明化效果,代表性方法是 CLARITY^[60]技术、PACT^[61-64]技术、SWITCH^[65]技术和 SHIELD 技术^[66]。该类组织透明方法对组织的透明效果较好,但是需要较长时间对组织进行脱脂处理,操作流程复杂。

在对样本进行光透明化处理后,可利用 LSFM 实现对鼠脑等大尺寸样本的快速成像。LSFM 原理如图 2 所示。LSFM 与传统显微镜有着显著的区别,在 LSFM 中照明光路和探测光路是分开的:照明光路成薄片状照明光从侧面照射样本从而实现选择性的荧光激发;探测光路的物镜光轴垂直于照明光片,物镜的焦面与光片重合,保证照明光片所激发的荧光信号被物镜收集,并最终被面阵探测器所记录。LSFM 的轴向分辨率由光片的厚度和探测物镜的数值孔径(NA)共同决定。与传统显微镜相比,LSFM 具备良好的光学层析能力,能够极大程度地减少非必要荧光激发。为了覆盖小鼠全脑的成像范围,LSFM 通常采用更低 NA 的物镜,以数微米的体素分辨率进行宽场成像探测,因此成像速度快于其他全脑显微光学成像技术。此外,LSFM 还可对同一样本进行多角度重复成像^[67-69],通过多视角反卷积等算法^[70-71]提升分辨率和图像对比度。

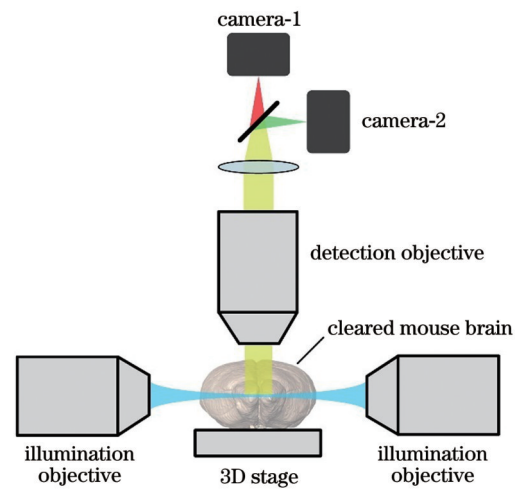


图 2 光片荧光显微镜原理图

Fig. 2 Schematic of light-sheet fluorescence microscopy

光片照明的概念早在 100 多年前就被提出^[72],但直到最近的 20 多年来,LSFM 技术才得到快速发展与进步。2004 年,Huisken 等^[73]首次提出选择性平面照明显微镜(SPIM),实现了对毫米尺寸青鳉鱼和果蝇胚胎的快速成像,轴向分辨率优于 6 μm。2007 年,Dodt 等^[74]发明的超级显微镜采用双侧照明的光路,首

次实现对透明鼠脑的全脑成像,获取了 Thy1-GFP 转基因小鼠全脑的成像结果。2008年,Keller等^[75]发展了数字扫描光片荧光显微镜(DSLM),通过快速扫描光束的方式形成虚拟照明光片,提升了照明光片的均匀性、照明效率和成像质量。2012年,Silvestri等^[76]提出了共聚焦光片显微镜(CLSM),采用与DSLM类似的快速扫描光束方式形成虚拟光片,并使用狭缝光阑过滤了大量非弹道的荧光信号,进一步提升系统的背景抑制能力。但该系统需要三套扫描装置和复杂的同步控制,否则探测到的荧光信号将极大衰减。同年,Baumgart等^[77]提出了一种基于科学级互补金属氧化物半导体(sCMOS)相机卷帘门模式的CLSM。该方法不使用物理狭缝光阑和重扫描装置,直接将sCMOS相机探测面与虚拟光片共轭,利用相机卷帘门模式下逐行曝光的特点来实现照明光束与相机对应行像素的同步曝光,并且相机的每一行像素都可充当狭缝光阑的角色来隔离背景光。2019年,Chakraborty等^[78]提出了轴向扫描光片显微镜(ASLM),通过在照明光路实现无像差的快速远程聚焦,配合相机卷帘门模式下逐行曝光,在数毫米长的透明化小鼠骨髓样本上可实现最高约300 nm的各向同性分辨率成像。2022年,Glaser等^[79]发展了一种混合开顶式光片显微镜(OTLS),结合了非正交双物镜和开顶式光片系统架构,可根据不同的成像需求对各类组织经透明处理的大尺寸样本灵活地进行多尺度高通量成像,提供了一种高效的解决方案。

2020年,西湖大学高亮团队Chen等^[80]发展的拼接光片照明显微镜(Tiling LSM),将前期发展的拼接光片技术^[81]应用于厘米尺寸光透明化的鼠脑等样本,可实现不同体素采样率的快速成像。该技术的核心是使用高数值孔径照明物镜形成薄而窄的小照明光片,并利用空间光调制器将照明光片在整个成像视野中快速移动,达到多个小照明光片“拼接”成为大照明光片的效果,在增加视场范围的同时保证了较高的轴向分辨率。2019年,中国科学技术大学毕国强团队Wang等^[82]发展了高速三维荧光成像技术ViSoR,通过倾斜截面扫描光束照明与同步成像实现了对透明鼠脑样本切片连续运动时的快速图像采集。2021年该团队利用此成像技术,将猕猴全脑切成约250张300 μm厚度的切片后分别进行光透明化处理和快速扫描成像,再通过数据配准方法实现不同切片数据之间的拼接^[83]。这种方案避免了猕猴全脑难以直接进行光透明化处理的问题,能够以1 μm×1 μm×2.5 μm的体素采样率实现对猕猴全脑的成像,但同时存在切片之间的数据损失、非刚性形变和三维配准的难题。2021年,清华大学郭增才团队Zhang等^[84]研制了多尺度光片荧光显微镜(mLSFM),通过自动调节探测光路放大率和光片厚度可方便地实现不同体素采样率的成像,同时,该技术在照明光路中采用可变焦透镜,结合探测相机的卷

帘门模式的同步曝光,优化提升了视场范围内轴向分辨率的均一性。该技术既可直接对透明样本进行整体快速成像,也可选择利用振动切片去除顶层已成像的样本,改善了大样本整体成像质量不均匀的问题,但透明后样本机械性能不佳,切片前后的样本形变导致轴向数据块之间存在错位,需要在上下层数据间保留一定比例的冗余采集以保证后期配准与校正。

总体而言,LSFM的成像速度较快,对于小鼠全脑样本,一般可在数小时或更短时间内完成微米水平分辨率的快速成像。由于照明光片仅激发光片内的荧光信号,因此,LSFM在实现良好光学层析效果的同时可保证较小的光漂白和光毒性。但与此同时,LSFM一般具有以下缺点:(1)成像质量随着成像深度的增加而退化,其成像分辨率在样本深处会显著下降,在大尺寸样本完整成像中往往无法获得样本深处的精细信号;(2)照明光片的厚度与照明视场的大小成反相关,在大尺寸样本完整成像时需要使用低数值孔径的物镜,导致光片厚度增加,轴向分辨率降低。因此,LSFM技术非常适合于全脑范围胞体分布成像等分辨率要求较低的研究,或对局部小区域实现精细成像,仍难以对完整鼠脑等大尺寸样本实现亚微米分辨率的均一、精细成像。

3 基于机械切削的全脑显微光学成像方法

基于机械切削的全脑显微光学成像方法将光学层析成像技术与组织切削技术相结合:每次扫描获取整个样本断面浅层部分的层析图像后,利用刀具切削掉样本表面已成像的部分,通过不断循环“样本断面成像-切削”过程,即可实现对厘米尺寸大样本的三维精细结构信息获取。这种技术方案的优势在于成像位置始终处于散射较低的样本浅层,可保证大尺寸样本整体均匀一致的成像质量。此种技术方案的代表包括双光子序列断层成像(STP)技术、块表面序列成像(FAST)技术和显微光学切片断层成像(MOST)系列技术。

3.1 双光子序列断层成像

2007年,Ragan等^[85]发展的双光子组织成像仪首次将双光子显微镜与石蜡切片技术结合,以0.78 μm×0.78 μm×2 μm的体素采样率实现了对完整小鼠心脏的成像。2012年,进一步发展的STP^[86]技术将高速双光子成像与振动切片技术相结合,利用双光子点扫描成像以马赛克拼接方式获取样本浅层部分的层析图像,随后通过振动切片去除表层已成像的样本组织。STP技术原理如图3所示。STP技术拥有较高的横向采样率(2 μm、1 μm 和 0.5 μm 可选),并且样本的琼脂糖包埋流程简单,不会导致荧光信号衰减和样本形变。但为了缩短成像时间,其轴向采样间隔达到50 μm以上,导致无法完成三维连续信号的追踪。2016年,

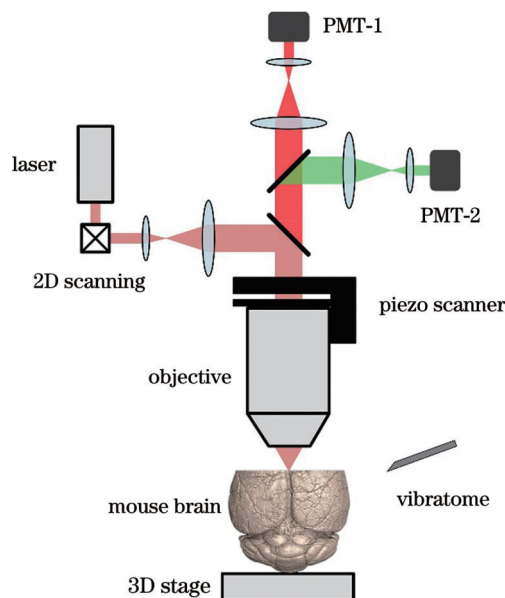


图 3 双光子序列断层成像原理图

Fig. 3 Schematic of serial two-photon tomography

Econo 等^[87]通过使用共振式扫描振镜和更高的激发光强度,将 STP 系统扫描成像的速度进一步提升,并通过优化鼠脑组织透明化处理方法,在将成像深度提高到 200 μm 以上的同时亦可实现振动切片,最终可在 8~10 天内获得 $0.3 \mu\text{m} \times 0.3 \mu\text{m} \times 1 \mu\text{m}$ 的高分辨率小鼠全脑数据。该技术用于 MouseLight 项目中以实现单个神经元完整形态的重建^[15]。2019 年,Abdeladim 等^[88]发展了一种彩色多光子断层成像技术 ChroMS,利用两种波长的激光器和波长混合技术完成多色激发,并使用四个探测器实现四个通道同时探测。该技术可实现对“脑虹”小鼠的多色全脑成像,但受限于较慢的点扫描速度,全脑多色成像的轴向采样间隔高达 100 μm 。

由于双光子串行扫描的工作方式很大程度上限制了成像通量,STP 技术为缩短成像时间,一般的典型应用为轴向数十微米至 100 μm 的间隔采样成像,牺牲了三维空间数据的连续性。由于样本琼脂糖包埋流程简单无形变的特点,使得 STP 在中尺度解剖中十分有用,目前已得到大量各类型小鼠全脑的图像数据集^[28,89-90]。MouseLight 项目采用改进后的 STP 技术可实现全脑亚微米分辨率的精细成像,但透明化后样本的机械性能不佳,导致厚组织切片产生的轴向数据块之间缺乏天然自配准特性,需要后期校正。

3.2 块表面序列成像

与 STP 技术类似,2017 年 Seiriki 等提出的 FAST^[91-92]技术同样采用琼脂糖包埋方式并利用振动切片机实现厚度为 50~80 μm 的快速切片。不同之处在于 FAST 采用转盘共聚焦实现对浅层约 100 μm 厚度内组织的层析成像,能够以 $0.7 \mu\text{m} \times 0.7 \mu\text{m} \times 5 \mu\text{m}$ 的体素采样率在 2.4 h 内完成小鼠全脑单色成像,并可使用三种不同波长激发光依次照明样本,完成三色成

像。转盘共聚焦具有与传统共聚焦显微镜相当的光学层析能力,同时结合多点并行照明和探测,使其拥有较高的成像速度。FAST 技术原理如图 4 所示。采用该技术可实现对小鼠脑、狨猴脑和人脑脑块样本的快速胞体分辨水平成像。

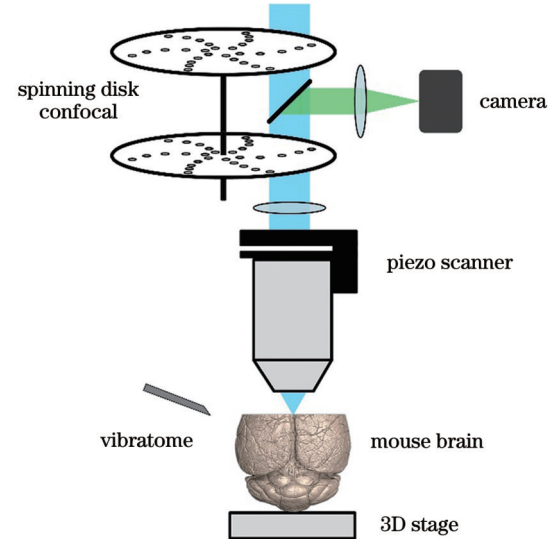


图 4 块表面序列成像原理图

Fig. 4 Schematic of block-face serial microscopy tomography

2021 年清华大学郭增才团队 Chen 等^[93]提出了基于稀疏成像+重建的断层成像(SMART)技术。该技术同样采用转盘共聚焦结合振动切片的成像系统,通过低分辨率成像结果判定当前区域是否存在荧光信号并结合“稀疏标记信号的连续性”这一特点来缩小下一次的扫描范围,实现了对光透明化稀疏标记小鼠的快速精细成像。该技术是通过优化采集策略来缩小成像范围而非提升成像通量;低分辨成像可能造成弱信号未被识别,造成信号缺失;并且透明后样本机械性能不佳,切片前后的轴向数据块之间缺乏天然自配准特性,需要后期校正。

3.3 显微光学切片断层成像系列技术

2010 年,华中科技大学作者所在实验室提出 MOST^[94]技术,将反射式切片成像和全自动精密切削相结合,利用金刚石刀具对树脂包埋的鼠脑样本进行 1 μm 厚度连续切片,同时对刀刃上所形成的样本切片进行线扫描成像,首次获取了体素分辨率小于 1 μm^3 的小鼠全脑高尔基染色数据集。这种边切片边成像的方式,以机械切削确定轴向成像深度,避免了成像面以外区域信号的干扰,保证了所获图像的质量。该方法还利用组织吸收率的差异,在尼氏染色啮齿类动物完整脑上同时获取了细胞构筑与血管网络两种信息^[21-22,95]。2013 年所发展的荧光显微光学切片断层成像(fMOST)^[96]技术在 MOST 系统边切片边成像的基础上,发展了适合于荧光蛋白标记鼠脑的树脂包埋方法,并利用基于声光偏转扫描的共聚焦荧光显微镜实现了长时间的稳定成像,成功获取了 1 μm^3 体素分辨率的小

鼠全脑数据集，并首次展示了全脑范围内单个神经元无中断长程轴突投射的追踪结果^[12]。同年所提出的双光子荧光显微光学切片断层成像(2p-fMOST)^[97]技术采用对样本块表面进行成像的方式，利用金刚石刀具将树脂包埋的鼠脑样本加工形成平整的断面，再通过双光子成像获取浅层组织的层析图像，通过交替进行切片和成像过程即可获得微米分辨率的小鼠全脑数据集。此种工作方式使成像与切削分离，避免了成像质量对切削质量的依赖，进一步提高了系统的稳定性。

2016年发展的结构光照明荧光显微光学切片断层成像(SI-fMOST)^[98]技术采用结构光照明成像^[99]方式，通过马赛克扫描拼接实现对样本块整个断面的高通量成像层析，结合样本成像过程中的实时染色技术，可在3天内以 $0.32\text{ }\mu\text{m}\times 0.32\text{ }\mu\text{m}\times 2\text{ }\mu\text{m}$ 的体素采样率完成小鼠全脑双色成像，同时提供神经元投射和细胞构筑定位信息。2017年提出一种可实现自动化切片收集的快速全脑光学成像系统^[100]，通过快速全脑成像筛选出目标脑区并对收集的切片进行免疫染色，实现了特定神经环路分子表型信息的高效获取。同年发展的深低温显微光学切片断层成像(cryo-MOST)^[101]技术可实现深低温环境中的高分辨率光学成像，并首次实现了全脑老年斑分布无标记获取。

2017年发展的双模式显微光学切片断层成像(dMOST)^[102]技术，利用三窗口二色镜，巧妙地实现了对荧光和反射双模式信号的同时探测，实现了对高尔基染色灵长类脑组织的神经元形态与荧光复染共定位细胞构筑信息的同时获取。2018年发展的光片照明显微光学切片断层成像技术HLTP^[103]将光片照明成像与振动切片相结合，利用光片照明实现对样本块表面浅层部分的成像，无需对样本进行光透明化处理。该技术可在5 h内以 $1.3\text{ }\mu\text{m}\times 1.3\text{ }\mu\text{m}\times 0.92\text{ }\mu\text{m}$ 的体素采样率完成小鼠全脑成像，适于全脑范围的快速细胞分辨水平成像。

2018年首次提出利用深度学习实现光学层析的新方法^[104]，并将其改良应用到fMOST技术中，在2020年提出了基于深度学习的fMOST(DL-fMOST)^[105]新

技术，在SI-fMOST原有构架下将成像时间缩短2/3，并克服了结构光照明成像图像噪声大的不足，提升了图像质量。

2021年发展的化学层析荧光显微光学切片断层成像(CS-fMOST)^[106]技术利用化学层析原理^[107]，在样本制备过程中抑制荧光蛋白信号并在成像过程中实时重新激活样本断面部分的荧光，实现了高通量全脑范围突触分辨水平精细成像。同年提出了线照明调制(LiMo)显微术，利用线照明的高斯光强分布作为天然的照明调制，以简洁的离轴多线并行探测与线照明扫描成像结合，仅需一步减法即可有效去除背景干扰。该技术的背景抑制能力优于共聚焦等传统显微成像技术，克服了传统结构光照明成像中存在残留调制伪影的固有缺陷，并具有线扫描对大范围样本成像通量高的优点，解决了传统荧光显微光学层析成像方法无法同时兼顾高分辨率、高通量和高清晰度的问题。基于该技术迭代升级的高清荧光显微光学切片断层成像(HD-fMOST)^[108]技术，以 $0.3\text{ }\mu\text{m}\times 0.3\text{ }\mu\text{m}\times 1\text{ }\mu\text{m}$ 的体素分辨率在5天内获取小鼠全脑高清双色数据集，原始数据平均信背比(SBR)高达110。出色的成像质量证明HD-fMOST技术将全脑光学成像技术从高分辨率提升到高清晰度的新标准，为解决限制其推广应用的大数据瓶颈问题提供了全新的途径。

2022年发展了针对猕猴全脑的亚细胞分辨精细结构成像的新技术^[109]，将猕猴全脑的水凝胶包埋、轴突分辨的自动化成像和PB量级数据处理方法结合，能够以 $0.65\text{ }\mu\text{m}\times 0.65\text{ }\mu\text{m}\times 3\text{ }\mu\text{m}$ 的体素分辨率对猕猴全脑进行自动化的三维连续数据获取，并展示了猕猴全脑的三维细胞构筑信息和前额叶单神经元的全脑投射信息。同年发展了一种低温荧光显微光学切片断层成像(cryo-fMOST)^[110]技术，通过热电级联冷却的方式构建稳定的低温成像环境，能够以亚微米体素分辨率高保真地获取冰冻包埋器官的精细解剖结构并保持其生化信息，可进一步对收集到的已成像冰冻切片进行多组学测量，有望用于空间多组学的研究。

图5所示为几种代表性的MOST技术的原理图，

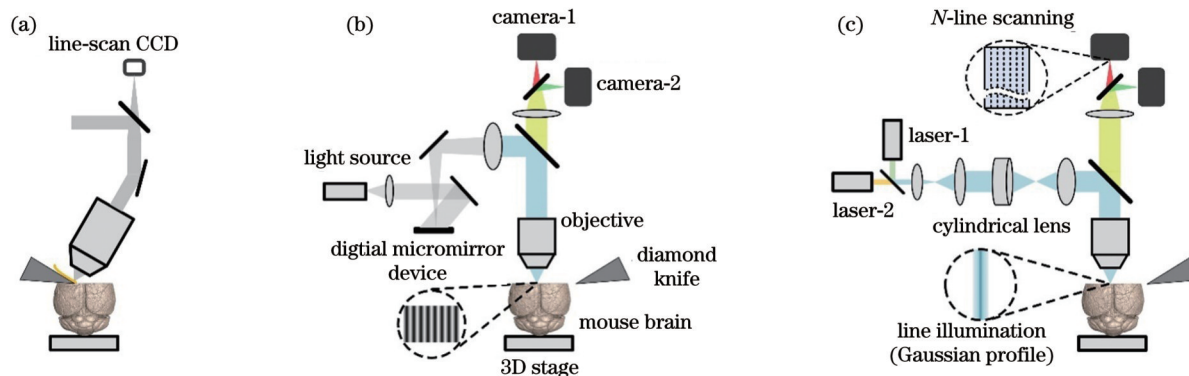


图5 几种代表性的 MOST 技术的原理图。(a) MOST；(b) SI-fMOST；(c) HD-fMOST

Fig. 5 Schematic of several typical MOST technologies. (a) MOST; (b) SI-fMOST; (c) HD-fMOST

分别为MOST、SI-fMOST和HD-fMOST。

总体而言,MOST系列技术将完整脑样本包埋制备、显微光学成像和自动化精密切削技术相结合,形成了独具特色的技体系并持续不断地发明新技术新工具。MOST系列技术为全脑介观神经联接图谱绘制提供了在全脑样品的全部空间中遍历每个像素的高分辨率光学成像方法,所采集的数据集均表现

出数据完整、三维可重建、分辨率高和数据质量好等特点,可以对神经元完整形态、神经元分布、血管网络等解剖结构在精确定位下进行定量的形态学分析与比较。

4 总结与展望

表1比较了不同全脑显微光学成像方法的性能比较。

Table 1 Performance comparison of different methods of whole-brain optical imaging

Type	Typical method	Sample preparation/slicing method	Typical voxel size	Data collection time	Suitable range of application	Whole-brain 3D dataset quality and consistency
LSFM	Ultramicroscopy 2007 ^[74]	Clearing	100–600 optical sections	6–8 h/mouse brain	Soma distribution, vascular network	★ Poor light sheet quality; inconsistent resolution, severe loss of deep quality
	Tiling LSM 2020 ^[80]	Clearing	2.6 μm×2.6 μm×6 μm (overall), 0.3 μm×0.3 μm×1 μm (local)	5 h/mouse brain (2.6 μm×2.6 μm×6 μm)	Soma distribution, vascular network, fine morphology of local neurons (axons, dendrites)	★★ Inconsistent resolution, loss of deep quality
	mLSFM 2021 ^[84]	Clearing, vibrating sectioning	0.8 μm×0.8 μm×5 μm (overall), 0.3 μm×0.3 μm×1 μm (local)	95 min/mouse brain (0.8 μm×0.8 μm×5 μm)	Soma distribution, vascular network, fine morphology of local neurons (axons, dendrites)	★★ Inconsistent resolution; poor slicing performance and deformation
	VISoR 2021 ^[83]	Clearing	1 μm×1 μm×2.5 μm	94 h (macaque brain slices)	Soma distribution, vascular network, neuronal axonal projections	★ Data loss between slices, difficult to register
STP	STP 2012 ^[86]	Agarose-embedding, vibrating sectioning	0.5 μm×0.5 μm×50 μm	24 h/mouse brain	Soma distribution, neuronal axonal projections	★★★ Consistent resolution and image quality; discontinuous Z-interval sampling
	MouseLight 2016 ^[87]	Clearing, vibrating sectioning	0.3 μm×0.3 μm×1 μm	8–10 days/mouse brain	Soma distribution, vascular and capillary network, complete fine morphology of neurons (axons, dendrites, spines)	★★★★ Poor slicing performance and deformation
FAST	FAST 2017 ^[91]	Agarose-embedding, vibrating sectioning	0.7 μm×0.7 μm×5 μm	2.4–10 h/mouse brain	Soma distribution, vascular network, neuronal axonal projections	★★ Consistent resolution and image quality
	SMART 2021 ^[93]	Clearing, vibrating sectioning	0.7 μm×0.7 μm×30 μm (overall), 0.3 μm×0.3 μm×1 μm (local)	20 h/part of mouse brain (0.3 μm×0.3 μm×1 μm)	Soma distribution, vascular network, fine morphology of local neurons (axons, dendrites)	★★ Poor slicing performance and deformation; weak signals may go unrecognized and missing
MOST	MOST 2010 ^[94]	Nissl/Golgi staining, resin-embedded sectioning	0.33 μm×0.33 μm×1 μm	242 h/mouse brain	Nissl stained soma, vascular and capillary network, Golgi stained neuron	★★ Consistent resolution and image quality; slight data loss between slice strips

续表

Type	Typical method	Sample preparation/ slicing method	Typical voxel size	Data collection time	Suitable range of application	Whole-brain 3D dataset quality and consistency
	SI-fMOST 2016 ^[98]	Resin-embedded sectioning	0.32 μm × 0.32 μm × 2 μm	3 days/mouse brain	Soma distribution, vascular and capillary network, complete fine morphology of neurons (axons, dendrites)	★★★★
MOST	HD-fMOST 2021 ^[108]	Resin-embedded sectioning	0.32 μm × 0.32 μm × 1 μm	111 h/mouse brain	Soma distribution, vascular and capillary network, complete fine morphology of neurons (axons, dendrites, spines)	★★★★★
	Macaque brain imaging 2022 ^[109]	Hydrogel embedding, vibrating sectioning	0.65 μm × 0.65 μm × 3 μm	70 days/ macaque brain	Soma distribution, vascular network, neuronal axonal projections	★★★

这些全脑显微光学成像新兴技术实现了前所未有的分辨率、成像速度和成像范围,使得研究全脑神经网络结构和功能成为可能,已逐渐成为脑科学以及其他相关学科的研究利器,并将继续发展成为更具普适性的科研工具,从而展现更多的应用价值。神经科学家对新技术的需求也促进了全脑显微光学成像技术从实验室原理样机到商业设备的快速发展,其中部分技术已转化成为商业光学成像设备,例如基于LSFM的Zeiss(德国)、锘海(中国)、Bruker(德国)、LaVision(德国)显微镜,基于STP的TissueVision(美国)显微镜,基于MOST系列技术的沃亿生物(中国)BioMapping系列设备,等等。可以看出,在全脑光学成像这一显微镜细分领域,我国在技术研发与设备制造方面与国外高水平研究机构和公司相比已具有一定的竞争实力,甚至在部分特色技术上取得了领先。但整体来说,国产光学成像设备的产品综合实力与国外品牌相比还存在较大差距,探测器、精密平移台、激光光源和配套数据分析处理软件等核心零部件严重依赖进口。我国在全脑光学成像技术上仍在持续投入、迅速发展,将不断积累相关研发经验,有望在高端光学影像设备的国产化上做出成绩,早日实现光学显微的中国制造。

绘制全脑介观神经联接图谱不仅需要大范围高分辨率的成像技术,还需同时发展样本标记与制备、海量数据存储处理与可视化等方法。近些年来,各种病毒示踪工具的发展大大推动了神经环路的结构解析,病毒已经成为环路示踪领域最常用的工具^[111-112]。嗜神经病毒示踪技术可在神经元内高效表达荧光蛋白,不同病毒载体可通过携带不同报告基因或特定功能元件,实现神经元精细形态标记、神经网络的结构可视化

或特定功能的标记、细胞类型特异标记等标记效果,从而“点亮”神经环路。标记制备的全脑样本经过介观分辨水平成像后,最终形成巨量研究数据,例如一个小鼠脑以亚微米体素分辨率成像可产生约10 TB数据。如何实现海量全脑成像数据的处理和分析并从中提取知识,很可能成为脑科学研究中的一个瓶颈^[113]。不同来源、不同标记方式的介观分辨脑图谱数据具有多层次、多类型、多形态的特点,是世界上最复杂的图像大数据,针对该类数据的处理和分析需面临以下挑战^[114]:如何实现复杂形态神经元的准确识别和重建^[115];如何建立标准的全脑坐标体系并实现多组学信息的整合^[116];如何构建硬件计算平台实现海量数据的高效存储、计算和传输;如何将跨越多个尺度的各类数据进行可视化展示。

全脑显微光学成像技术的发展极大地促进了全脑介观神经联接图谱数据的采集与分析,为神经科学领域开启新篇章,但因其复杂性,面向完整全脑的研究还有待进一步探索。另外,对于人脑高级功能和相应药物的研究,目前采用的啮齿动物样本有明显局限性。非人灵长类作为与人类最为接近的物种,对于研究人脑的认知行为、疾病机制和治疗手段有着极其重要的价值^[117]。日本的Brain/MINDS脑计划选取猕猴作为重要动物模型,对猕猴脑的结构和功能成像是整个脑计划的三大研究内容之一^[118]。中国脑计划提出使用更高等的猕猴作为重要的动物模型,并建立转基因模型和帕金森氏病等各类疾病模型^[11]。但猴脑的研究难度远大于小鼠脑:小鼠脑的质量仅为0.42 g左右,神经元的数目约为7000万;猕猴脑的质量为7.78 g左右,约为小鼠脑的20倍,神经元的数目达6亿3000万;而猕猴脑的质量更是达

到了87.35 g左右,约为小鼠脑的200倍,神经元的数量达63亿7000万^[119]。因此,非人灵长类的脑研究对于样本标记制备、成像技术和大数据处理等方面均提出了极大的挑战,之后的研究必须更加系统化并融合多学科的技术和方法。在成像手段上,面对扩大了3个数量级的三维成像范围,如何解决成像分辨率与成像通量的相互制约,使得完整人脑的高分辨全脑三维数据采集成为可能,是未来需要重点关注的技术难点之一,需要探索全新的策略与思路来寻求解决方案。

在与生物、机械、电子、工程、化学、计算机等多领域的跨学科合作中,全脑显微光学成像技术将进一步蓬勃发展,在脑科学中展示其独特的应用价值,共同完成绘制介观脑联接图谱的奋斗目标。相信这一宏大研究计划的实践,将极大促进我们对脑的认识和理解,助力人工智能技术的发展。

参考文献

- [1] Petreanu L, Mao T Y, Sternson S M, et al. The subcellular organization of neocortical excitatory connections[J]. *Nature*, 2009, 457(7233): 1142-1145.
- [2] Miyamichi K, Amat F, Moussavi F, et al. Cortical representations of olfactory input by trans-synaptic tracing[J]. *Nature*, 2011, 472(7342): 191-196.
- [3] Koch C, Reid R C. Observatories of the mind[J]. *Nature*, 2012, 483(7390): 397-398.
- [4] Snyder E Y, Yoon C, Flax J D, et al. Multipotent neural precursors can differentiate toward replacement of neurons undergoing targeted apoptotic degeneration in adult mouse neocortex[J]. *Proceedings of the National Academy of Sciences of the United States of America*, 1997, 94(21): 11663-11668.
- [5] Helmchen F, Denk W. Deep tissue two-photon microscopy[J]. *Nature Methods*, 2005, 2(12): 932-940.
- [6] Conchello J A, Lichtman J W. Optical sectioning microscopy[J]. *Nature Methods*, 2005, 2(12): 920-931.
- [7] Mertz J. Optical sectioning microscopy with planar or structured illumination[J]. *Nature Methods*, 2011, 8(10): 811-819.
- [8] 王潇, 涂世杰, 刘鑫, 等. 三维超分辨显微成像技术的研究进展及展望[J]. 激光与光电子学进展, 2021, 58(22): 2200001.
- Wang X, Tu S J, Liu X, et al. Advance and prospect for three-dimensional super-resolution microscopy[J]. *Laser & Optoelectronics Progress*, 2021, 58(22): 2200001.
- [9] 刘智, 罗泽伟, 王正印, 等. 基于结构照明的超分辨荧光显微成像重建算法[J]. 中国激光, 2021, 48(3): 0307001.
- Liu Z, Luo Z W, Wang Z Y, et al. Super-resolution fluorescence microscopy image reconstruction algorithm based on structured illumination[J]. *Chinese Journal of Lasers*, 2021, 48(3): 0307001.
- [10] 李浩宇, 曲丽颖, 华子杰, 等. 基于深度学习的荧光显微成像技术及应用[J]. 激光与光电子学进展, 2021, 58(18): 1811007.
- Li H Y, Qu L Y, Hua Z J, et al. Deep learning based fluorescence microscopy imaging technologies and applications[J]. *Laser & Optoelectronics Progress*, 2021, 58(18): 1811007.
- [11] Poo M M, Du J L, Ip N Y, et al. China brain project: basic neuroscience, brain diseases, and brain-inspired computing[J]. *Neuron*, 2016, 92(3): 591-596.
- [12] Osten P, Margrie T W. Mapping brain circuitry with a light microscope[J]. *Nature Methods*, 2013, 10(6): 515-523.
- [13] Guo C D, Long B, Hu Y R, et al. Early-stage reduction of the dendritic complexity in basolateral amygdala of a transgenic mouse model of Alzheimer's disease[J]. *Biochemical and Biophysical Research Communications*, 2017, 486(3): 679-685.
- [14] Guo C D, Peng J, Zhang Y L, et al. Single-axon level morphological analysis of corticofugal projection neurons in mouse barrel field[J]. *Scientific Reports*, 2017, 7(1): 2846.
- [15] Winnubst J, Bas E, Ferreira T A, et al. Reconstruction of 1,000 projection neurons reveals new cell types and organization of long-range connectivity in the mouse brain[J]. *Cell*, 2019, 179(1): 268-281.
- [16] Peng H C, Xie P, Liu L J, et al. Morphological diversity of single neurons in molecularly defined cell types[J]. *Nature*, 2021, 598(7879): 174-181.
- [17] Wang Q X, Ding S L, Li Y, et al. The Allen mouse brain common coordinate framework: a 3D reference atlas[J]. *Cell*, 2020, 181(4): 936-953.
- [18] Long B, Jiang T, Zhang J M, et al. Mapping the architecture of ferret brains at single-cell resolution[J]. *Frontiers in Neuroscience*, 2020, 14: 322.
- [19] Qu L, Li Y Y, Xie P, et al. Cross-modal coherent registration of whole mouse brains[J]. *Nature Methods*, 2022, 19(1): 111-118.
- [20] Feng Z, Li A A, Gong H, et al. Constructing the rodent stereotaxic brain atlas: a survey[J]. *Science China Life Sciences*, 2022, 65(1): 93-106.
- [21] Wu J P, He Y, Yang Z Q, et al. 3D BrainCV: simultaneous visualization and analysis of cells and capillaries in a whole mouse brain with one-micron voxel resolution[J]. *NeuroImage*, 2014, 87: 199-208.
- [22] Wu J P, Guo C D, Chen S B, et al. Direct 3D analyses reveal barrel-specific vascular distribution and cross-barrel branching in the mouse barrel cortex[J]. *Cerebral Cortex*, 2014, 26(1): 23-31.
- [23] Xiong B Y, Li A A, Lou Y, et al. Precise cerebral vascular atlas in stereotaxic coordinates of whole mouse brain[J]. *Frontiers in Neuroanatomy*, 2017, 11: 128.
- [24] Zhang X C, Yin X Z, Zhang J J, et al. High-resolution mapping of brain vasculature and its impairment in the hippocampus of Alzheimer's disease mice[J]. *National Science Review*, 2019, 6(6): 1223-1238.
- [25] Tang J, Zhu H, Tian X Y, et al. Extension of endocardium-derived vessels generate coronary arteries in neonates[J]. *Circulation Research*, 2022, 130(3): 352-365.
- [26] Yin X Z, Zhang X C, Zhang J J, et al. High-resolution digital panorama of multiple structures in whole brain of Alzheimer's disease mice[J]. *Frontiers in Neuroscience*, 2022, 16: 870520.
- [27] He X Z, Li X, Li Z H, et al. High-resolution 3D demonstration of regional heterogeneity in the glymphatic system[J]. *Journal of Cerebral Blood Flow and Metabolism*, 2022, 42(11): 2017-2031.
- [28] Oh S W, Harris J A, Ng L, et al. A mesoscale connectome of the mouse brain[J]. *Nature*, 2014, 508(7495): 207-214.
- [29] Callaway E M, Dong H W, Ecker J R, et al. A multimodal cell census and atlas of the mammalian primary motor cortex[J]. *Nature*, 2021, 598(7879): 86-102.
- [30] Muñoz-Castañeda R, Zingg B, Matho K S, et al. Cellular anatomy of the mouse primary motor cortex[J]. *Nature*, 2021, 598(7879): 159-166.
- [31] Foster N N, Barry J, Korobkova L, et al. The mouse cortico-basal ganglia-thalamic network[J]. *Nature*, 2021, 598(7879): 188-194.
- [32] Xu Z C, Feng Z, Zhao M T, et al. Whole-brain connectivity atlas of glutamatergic and gabaergic neurons in the mouse dorsal and median raphe nuclei[J]. *eLife*, 2021, 10: e65502.
- [33] Sun Q T, Zhang J P, Li A A, et al. Acetylcholine deficiency disrupts extratelencephalic projection neurons in the prefrontal cortex in a mouse model of Alzheimer's disease[J]. *Nature Communications*, 2022, 13: 998.
- [34] Richardson D S, Lichtman J W. Clarifying tissue clearing[J]. *Cell*, 2015, 162(2): 246-257.
- [35] Richardson D S, Guan W, Matsumoto K, et al. Tissue clearing [J]. *Nature Reviews Methods Primers*, 2021, 1: 84.

- [36] Tainaka K, Kuno A, Kubota S I, et al. Chemical principles in tissue clearing and staining protocols for whole-body cell profiling [J]. Annual Review of Cell and Developmental Biology, 2016, 32: 713-741.
- [37] Susaki E A, Ueda H R. Whole-body and whole-organ clearing and imaging techniques with single-cell resolution: toward organism-level systems biology in mammals[J]. Cell Chemical Biology, 2016, 23(1): 137-157.
- [38] Spalteholz W. Über das durchsichtigmachen von menschlichen und tierischen Präparaten und seine theoretischen Bedingungen, nebstanhang: über knochenfärbung[Z]. S. Hirzel Leipzig, 1914.
- [39] Ueda H R, Ertürk A, Chung K, et al. Tissue clearing and its applications in neuroscience[J]. Nature Reviews Neuroscience, 2020, 21(2): 61-79.
- [40] Ertürk A, Becker K, Jährling N, et al. Three-dimensional imaging of solvent-cleared organs using 3DISCO[J]. Nature Protocols, 2012, 7(11): 1983-1995.
- [41] Ertürk A, Mauch C P, Hellal F, et al. Three-dimensional imaging of the unsectioned adult spinal cord to assess axon regeneration and glial responses after injury[J]. Nature Medicine, 2012, 18(1): 166-171.
- [42] Renier N, Wu Z H, Simon DJ, et al. iDISCO: a simple, rapid method to immunolabel large tissue samples for volume imaging[J]. Cell, 2014, 159(4): 896-910.
- [43] Pan C C, Cai R Y, Quacquarelli F P, et al. Shrinkage-mediated imaging of entire organs and organisms using uDISCO[J]. Nature Methods, 2016, 13(10): 859-867.
- [44] Qi Y S, Yu T T, Xu J Y, et al. FDISCO: advanced solvent-based clearing method for imaging whole organs[J]. Science Advances, 2019, 5(1): eaau8355.
- [45] Cai R Y, Pan C C, Ghasemigharagoz A, et al. Panoptic imaging of transparent mice reveals whole-body neuronal projections and skull-meninges connections[J]. Nature Neuroscience, 2019, 22(2): 317-327.
- [46] Hahn C, Becker K, Saghafi S, et al. High-resolution imaging of fluorescent whole mouse brains using stabilised organic media (sDISCO)[J]. Journal of Biophotonics, 2019, 12(8): e201800368.
- [47] Jing D, Zhang S W, Luo W J, et al. Tissue clearing of both hard and soft tissue organs with the PEGASOS method[J]. Cell Research, 2018, 28(8): 803-818.
- [48] Ke M T, Fujimoto S, Imai T. SeeDB: a simple and morphology-preserving optical clearing agent for neuronal circuit reconstruction [J]. Nature Neuroscience, 2013, 16(8): 1154-1161.
- [49] Ke M T, Nakai Y, Fujimoto S, et al. Super-resolution mapping of neuronal circuitry with an index-optimized clearing agent[J]. Cell Reports, 2016, 14(11): 2718-2732.
- [50] Liu Y C, Chiang A S. High-resolution confocal imaging and three-dimensional rendering[J]. Methods, 2003, 30(1): 86-93.
- [51] Aoyagi Y, Kawakami R, Osanai H, et al. A rapid optical clearing protocol using 2, 2'-thiodiethanol for microscopic observation of fixed mouse brain[J]. PLoS One, 2015, 10(1): e0116280.
- [52] Zhu X P, Huang L M, Zheng Y, et al. Ultrafast optical clearing method for three-dimensional imaging with cellular resolution[J]. Proceedings of the National Academy of Sciences of the United States of America, 2019, 116(23): 11480-11489.
- [53] Hama H, Kurokawa H, Kawano H, et al. Scale: a chemical approach for fluorescence imaging and reconstruction of transparent mouse brain[J]. Nature Neuroscience, 2011, 14(11): 1481-1488.
- [54] Hama H, Hioki H, Namiki K, et al. ScaleS: an optical clearing palette for biological imaging[J]. Nature Neuroscience, 2015, 18(10): 1518-1529.
- [55] Yu T T, Zhu J T, Li Y S, et al. RTF: a rapid and versatile tissue optical clearing method[J]. Scientific Reports, 2018, 8: 1964.
- [56] Hou B, Zhang D, Zhao S, et al. Scalable and Dil-compatible optical clearance of the mammalian brain[J]. Frontiers in Neuroanatomy, 2015, 9: 19.
- [57] Chen L L, Li G Y, Li Y M, et al. UbasM: an effective balanced optical clearing method for intact biomedical imaging[J]. Scientific Reports, 2017, 7: 12218.
- [58] Susaki E A, Tainaka K, Perrin D, et al. Whole-brain imaging with single-cell resolution using chemical cocktails and computational analysis[J]. Cell, 2014, 157(3): 726-739.
- [59] Susaki E A, Tainaka K, Perrin D, et al. Advanced CUBIC protocols for whole-brain and whole-body clearing and imaging[J]. Nature Protocols, 2015, 10(11): 1709-1727.
- [60] Chung K, Wallace J, Kim S Y, et al. Structural and molecular interrogation of intact biological systems[J]. Nature, 2013, 497(7449): 332-337.
- [61] Yang B, Treweek J B, Kulkarni R P, et al. Single-cell phenotyping within transparent intact tissue through whole-body clearing[J]. Cell, 2014, 158(4): 945-958.
- [62] Treweek J B, Chan K Y, Flytzanis N C, et al. Whole-body tissue stabilization and selective extractions via tissue-hydrogel hybrids for high-resolution intact circuit mapping and phenotyping[J]. Nature Protocols, 2015, 10(11): 1860-1896.
- [63] Yu T T, Qi Y S, Zhu J T, et al. Elevated-temperature-induced acceleration of PACT clearing process of mouse brain tissue[J]. Scientific Reports, 2017, 7: 38848.
- [64] Perbellini F, Liu A K L, Watson S A, et al. Free-of-acrylamide SDS-based tissue clearing (FASTClear) for three dimensional visualization of myocardial tissue[J]. Scientific Reports, 2017, 7: 5188.
- [65] Murray E, Cho J H, Goodwin D, et al. Simple, scalable proteomic imaging for high-dimensional profiling of intact systems [J]. Cell, 2015, 163(6): 1500-1514.
- [66] Park Y G, Sohn C H, Chen R, et al. Protection of tissue physicochemical properties using polyfunctional crosslinkers[J]. Nature Biotechnology, 2019, 37(1): 73-83.
- [67] Krzic U, Gunther S, Saunders T E, et al. Multiview light-sheet microscope for rapid in toto imaging[J]. Nature Methods, 2012, 9(7): 730-733.
- [68] Chhetri R K, Amat F, Wan Y N, et al. Whole-animal functional and developmental imaging with isotropic spatial resolution[J]. Nature Methods, 2015, 12(12): 1171-1178.
- [69] Nie J, Liu S, Yu T T, et al. Fast, 3D isotropic imaging of whole mouse brain using multiangle-resolved subvoxel SPIM[J]. Advanced Science, 2019, 7(3): 1901891.
- [70] Swoger J, Verveer P, Greger K, et al. Multi-view image fusion improves resolution in three-dimensional microscopy[J]. Optics Express, 2007, 15(13): 8029-8042.
- [71] Preibisch S, Amat F, Stamataki E, et al. Efficient Bayesian-based multiview deconvolution[J]. Nature Methods, 2014, 11(6): 645-648.
- [72] Siedentopf H, Zsigmondy R. Über sichtbarmachung und größenbestimmung ultramikroskopischer teilchen, mit besonderer anwendung auf goldrubiengläser[J]. Annalen Der Physik, 1902, 315(1): 1-39.
- [73] Huisken J, Swoger J, del Bene F, et al. Optical sectioning deep inside live embryos by selective plane illumination microscopy[J]. Science, 2004, 305(5686): 1007-1009.
- [74] Dodt H U, Leischner U, Schierloh A, et al. Ultramicroscopy: three-dimensional visualization of neuronal networks in the whole mouse brain[J]. Nature Methods, 2007, 4(4): 331-336.
- [75] Keller P J, Schmidt A D, Wittbrodt J, et al. Reconstruction of zebrafish early embryonic development by scanned light sheet microscopy[J]. Science, 2008, 322(5904): 1065-1069.
- [76] Silvestri L, Bria A, Sacconi L, et al. Confocal light sheet microscopy: micron-scale neuroanatomy of the entire mouse brain [J]. Optics Express, 2012, 20(18): 20582-20598.
- [77] Baumgart E, Kubitscheck U. Scanned light sheet microscopy with confocal slit detection[J]. Optics Express, 2012, 20(19): 21805-21814.
- [78] Chakraborty T, Driscoll M K, Jeffery E, et al. Light-sheet microscopy of cleared tissues with isotropic, subcellular resolution

- [J]. *Nature Methods*, 2019, 16(11): 1109-1113.
- [79] Glaser A K, Bishop K W, Barner L A, et al. A hybrid open-top light-sheet microscope for versatile multi-scale imaging of cleared tissues[J]. *Nature Methods*, 2022, 19(5): 613-619.
- [80] Chen Y L, Li X L, Zhang D D, et al. A versatile tiling light sheet microscope for imaging of cleared tissues[J]. *Cell Reports*, 2020, 33(5): 108349.
- [81] Gao L. Extend the field of view of selective plan illumination microscopy by tiling the excitation light sheet[J]. *Optics Express*, 2015, 23(5): 6102-6111.
- [82] Wang H, Zhu Q Y, Ding L F, et al. Scalable volumetric imaging for ultrahigh-speed brain mapping at synaptic resolution[J]. *National Science Review*, 2019, 6(5): 982-992.
- [83] Xu F, Shen Y, Ding L F, et al. High-throughput mapping of a whole rhesus monkey brain at micrometer resolution[J]. *Nature Biotechnology*, 2021, 39(12): 1521-1528.
- [84] Zhang Z Z, Yao X, Yin X X, et al. Multi-scale light-sheet fluorescence microscopy for fast whole brain imaging[J]. *Frontiers in Neuroanatomy*, 2021, 15: 732464.
- [85] Ragan T, Sylvan J D, Kim K H, et al. High-resolution whole organ imaging using two-photon tissue cytometry[J]. *Journal of Biomedical Optics*, 2007, 12(1): 014015.
- [86] Ragan T, Kadirli L R, Venkataraju K U, et al. Serial two-photon tomography for automated *ex vivo* mouse brain imaging[J]. *Nature Methods*, 2012, 9(3): 255-258.
- [87] Economo M N, Clack N G, Lavis L D, et al. A platform for brain-wide imaging and reconstruction of individual neurons[J]. *eLife*, 2016, 5: e10566.
- [88] Abdeladim L, Matho K S, Clavreul S, et al. Multicolor multiscale brain imaging with chromatic multiphoton serial microscopy[J]. *Nature Communications*, 2019, 10: 1662.
- [89] Kim Y, Venkataraju K U, Pradhan K, et al. Mapping social behavior-induced brain activation at cellular resolution in the mouse [J]. *Cell Reports*, 2015, 10(2): 292-305.
- [90] Vousden D A, Epp J, Okuno H, et al. Whole-brain mapping of behaviourally induced neural activation in mice[J]. *Brain Structure and Function*, 2015, 220(4): 2043-2057.
- [91] Seiriki K, Kasai A, Hashimoto T, et al. High-speed and scalable whole-brain imaging in rodents and primates[J]. *Neuron*, 2017, 94 (6): 1085-1100.
- [92] Seiriki K, Kasai A, Nakazawa T, et al. Whole-brain block-face serial microscopy tomography at subcellular resolution using FAST [J]. *Nature Protocols*, 2019, 14(5): 1509-1529.
- [93] Chen H, Huang T Y, Yang Y X, et al. Sparse imaging and reconstruction tomography for high-speed high-resolution whole-brain imaging[J]. *Cell Reports Methods*, 2021, 1(6): 100089.
- [94] Li A A, Gong H, Zhang B, et al. Micro-optical sectioning tomography to obtain a high-resolution atlas of the mouse brain[J]. *Science*, 2010, 330(6009): 1404-1408.
- [95] Yuan J, Gong H, Li A A, et al. Visible rodent brain-wide networks at single-neuron resolution[J]. *Frontiers in Neuroanatomy*, 2015, 9: 70.
- [96] Gong H, Zeng S Q, Yan C, et al. Continuously tracing brain-wide long-distance axonal projections in mice at a one-micron voxel resolution[J]. *NeuroImage*, 2013, 74: 87-98.
- [97] Zheng T, Yang Z Q, Li A A, et al. Visualization of brain circuits using two-photon fluorescence micro-optical sectioning tomography [J]. *Optics Express*, 2013, 21(8): 9839-9850.
- [98] Gong H, Xu D L, Yuan J, et al. High-throughput dual-colour precision imaging for brain-wide connectome with cytoarchitectonic landmarks at the cellular level[J]. *Nature Communications*, 2016, 7: 12142.
- [99] Xu D L, Jiang T, Li A A, et al. Fast optical sectioning obtained by structured illumination microscopy using a digital mirror device [J]. *Journal of Biomedical Optics*, 2013, 18(6): 060503.
- [100] Jiang T, Long B, Gong H, et al. A platform for efficient identification of molecular phenotypes of brain-wide neural circuits [J]. *Scientific Reports*, 2017, 7: 13891.
- [101] Luo Y L, Wang A L, Liu M M, et al. Label-free brainwide visualization of senile plaque using cryo-micro-optical sectioning tomography[J]. *Optics Letters*, 2017, 42(21): 4247-4250.
- [102] Chen X, Zhang X Y, Zhong Q Y, et al. Simultaneous acquisition of neuronal morphology and cytoarchitecture in the same Golgi-stained brain[J]. *Biomedical Optics Express*, 2017, 9 (1): 230-244.
- [103] Yang X, Zhang Q, Huang F, et al. High-throughput light sheet tomography platform for automated fast imaging of whole mouse brain[J]. *Journal of Biophotonics*, 2018, 11(9): 201800047.
- [104] Zhang X Y, Chen Y F, Ning K F, et al. Deep learning optical-sectioning method[J]. *Optics Express*, 2018, 26(23): 30762-30772.
- [105] Ning K F, Zhang X Y, Gao X F, et al. Deep-learning-based whole-brain imaging at single-neuron resolution[J]. *Biomedical Optics Express*, 2020, 11(7): 3567-3584.
- [106] Wang X J, Xiong H Q, Liu Y R, et al. Chemical sectioning fluorescence tomography: high-throughput, high-contrast, multicolor, whole-brain imaging at subcellular resolution[J]. *Cell Reports*, 2021, 34(5): 108709.
- [107] Xiong H Q, Zhou Z Q, Zhu M Q, et al. Chemical reactivation of quenched fluorescent protein molecules enables resin-embedded fluorescence microimaging[J]. *Nature Communications*, 2014, 5: 3992.
- [108] Zhong Q Y, Li A A, Jin R, et al. High-definition imaging using line-illumination modulation microscopy[J]. *Nature Methods*, 2021, 18(3): 309-315.
- [109] Zhou C, Yang X Q, Wu S H, et al. Continuous subcellular resolution three-dimensional imaging on intact macaque brain[J]. *Science Bulletin*, 2022, 67(1): 85-96.
- [110] Deng L, Chen J W, Li Y F, et al. Cryo-fluorescence micro-optical sectioning tomography for volumetric imaging of various whole organs with subcellular resolution[J]. *iScience*, 2022, 25(8): 104805.
- [111] Qiu L Y, Zhang B, Gao Z H. Lighting up neural circuits by viral tracing[J]. *Neuroscience Bulletin*, 2022: 1-14.
- [112] Liu Q, Wu Y, Wang H D, et al. Viral tools for neural circuit tracing[J]. *Neuroscience Bulletin*, 2022: 1-11.
- [113] Frégnac Y. Big data and the industrialization of neuroscience: a safe roadmap for understanding the brain? [J]. *Science*, 2017, 358 (6362): 470-477.
- [114] Li A A, Guan Y, Gong H, et al. Challenges of processing and analyzing big data in mesoscopic whole-brain imaging[J]. *Genomics, Proteomics & Bioinformatics*, 2019, 17(4): 337-343.
- [115] Li S W, Quan T W, Zhou H, et al. Review of advances and prospects in neuron reconstruction[J]. *Chinese Science Bulletin*, 2019, 64(5/6): 532-545.
- [116] Bjerke I E, Øvsthus M, Papp E A, et al. Data integration through brain atlasing: human brain project tools and strategies[J]. *European Psychiatry*, 2018, 50: 70-76.
- [117] Huang Z J, Luo L Q. It takes the world to understand the brain[J]. *Science*, 2015, 350(6256): 42-44.
- [118] Okano H, Miyawaki A, Kasai K. Brain/MINDS: brain-mapping project in Japan[J]. *Philosophical Transactions of the Royal Society B: Biological Sciences*, 2015, 370(1668): 20140310.
- [119] Herculano-Houzel S. The human brain in numbers: a linearly scaled-up primate brain[J]. *Frontiers in Human Neuroscience*, 2009, 3: 31.

Whole-Brain Optical Imaging

Jiang Tao^{1,2}, Gong Hui^{1,2}, Luo Qingming^{1,2,3}, Yuan Jing^{1,2*}

¹HUST-Suzhou Institute of Brainsmatics, Suzhou 215000, Jiangsu, China;

²Wuhan National Laboratory for Optoelectronics, Huazhong University of Science and Technology, Wuhan 430074, Hubei, China;

³School of Biomedical Engineering, Hainan University, Haikou 570228, Hainan, China

Abstract

Significance The brain is one of the most complex systems, the culmination of evolution over billions of years of life. But until now we have not been able to accurately describe the mechanism of memory, thought and consciousness. Due to the lack of understanding of the structure and function of the brain, we have no effective drugs and treatments for neurological diseases such as schizophrenia, epilepsy, Alzheimer's disease, and Parkinson's disease. The structure of the brain is extremely complex and can be divided into different levels, such as brain lobes, neural circuits, neurons, synapses, and even molecules. The brain's powerful function stems from its huge number of nerve cells and their complex interconnections.

The mapping of whole-brain mesoscopic neural connections in model animals such as mice requires technical tools that can achieve large-scale acquisition of high-resolution three-dimensional data in the centimeter scale. Optical imaging methods can achieve sub-micron resolution in lateral direction and can realize "optical sectioning" by various means, which have the natural advantage of observing neural circuits at the mesoscopic level. In this review, we summarize the various kinds of whole-brain optical imaging methods developed in recent years and look forward to future technological development.

Progress Due to the scattering and absorption of biological tissues, the imaging depth of traditional optical methods is limited, and only tens of microns to hundreds of microns of the shallow layer of mouse brain can be imaged. To break through the limitation of imaging depth in biological tissues and achieve high voxel resolution and large-scale 3D imaging, optical microscopy must be combined with histological methods (Fig. 1).

Tissue clearing based whole-brain optical imaging methods are technologies that first clear biological tissues to improve optical imaging depth, and then use light-sheet fluorescence microscopy (LSFM) for rapid imaging (Fig. 2). For a whole mouse brain sample, rapid imaging of micrometer resolution can be completed in a few hours or less by LSFM. LSFM can achieve good optical sectioning with low photobleaching and phototoxicity. However, the imaging resolution of LSFM decreases significantly with the increase in the depth of the sample, and the resolution is lower when a large sample is fully imaged.

Mechanical sectioning based whole-brain optical imaging methods are a combination of optical sectioning and tissue cutting. After acquiring the images of the shallow part of sample each time, the sample surface is cut off with a knife. Through the continuous cycle of "imaging-cutting" process, the 3D fine structures of centimeter-size sample can be obtained. Representatives of this technology include serial two-photon tomography (STP), block-face serial microscopy tomography (FAST), and micro-optical sectioning tomography (MOST) series technologies.

STP combines high-speed two-photon imaging with vibrating sectioning, and can realize Z-interval sampling imaging of mouse brain (Fig. 3). With the use of resonant scanning galvanometer and higher excitation light intensity, the speed of STP imaging is further improved. By optimizing the mouse brain clearing method, the imaging depth can be improved to more than 200 μm . Finally, the high-resolution mouse brain data of $0.3 \mu\text{m} \times 0.3 \mu\text{m} \times 1 \mu\text{m}$ can be obtained within 8–10 days.

FAST uses spinning-disk confocal technology to image shallow tissues within a thickness of about 100 μm , and can complete monochromatic imaging of whole mouse brain within 2.4 h at a voxel size of $0.7 \mu\text{m} \times 0.7 \mu\text{m} \times 5 \mu\text{m}$ (Fig. 4). Sparse imaging and reconstruction tomography (SMART) uses low-resolution imaging results to determine whether there is fluorescence signal in the current region to narrow the next scan region, enabling rapid fine imaging of transparent sparse labeled mouse brain.

MOST uses a diamond knife to perform continuous sectioning of 1 μm thickness of resin-embedded mouse brain samples, and at the same time performs line scanning imaging of sample sections on the blade edge (Fig. 5). The mouse brain Golgi staining dataset with a voxel size of less than 1 μm^3 has been acquired for the first time. Structured illumination fluorescence micro-optical sectioning tomography (SI-fMOST) adopts structured illumination method to achieve high-throughput imaging of the sample block-face by mosaic scan stitching (Fig. 5). Combined with real-time staining, dual-color imaging of mouse brain can be completed in 3 days with voxel size of $0.32 \mu\text{m} \times 0.32 \mu\text{m} \times 2 \mu\text{m}$. High-definition fluorescence micro-optical sectioning tomography (HD-fMOST) uses the Gaussian intensity distribution of line illumination as a natural modulation, and can effectively remove background through simple subtraction (Fig. 5). The MOST series technologies combine embedding brain samples, micro-optical imaging and automatic precision cutting to form a unique technical system. The collected datasets are characterized by excellent integrity, high resolution, and good quality.

Conclusions and Prospects The whole-brain imaging technologies achieve unprecedented resolution, imaging speed and imaging

range, making it possible to study the whole-brain circuit network. These technologies have gradually become a powerful tool in neuroscience and will continue to develop into more universal research tools, thus showing more application value.

To map neural circuits, it is necessary not only to develop imaging technology, but also to develop methods such as sample labeling and preparation, massive data storage, processing, and visualization. In recent years, the development of various virus tracing tools has promoted the labeling of neural circuits. But how to process and analyze massive whole-brain imaging data and extract knowledge from it is likely to become a bottleneck.

As the closest species to humans, non-human primates are of great value for the study of cognitive behavior, disease mechanism and treatment. However, the weight of macaque brain is about 200 times that of a mouse brain, which poses great challenges to sample labeling preparation, imaging technology and big data processing.

Through interdisciplinary cooperation, whole-brain optical imaging will further flourish, demonstrate its unique application value in neuroscience, promote our knowledge and understanding of the brain, and contribute to the development of artificial intelligence technology.

Key words bio-optics; whole-brain optical imaging; optical tomography; micrometer resolution; brain connectome; neural circuits; neuron